The cytoplasmic tail of human mannosidase Man1b1 contributes to catalysis-independent quality control of misfolded alpha1-antitrypsin

Ashlee H. Sun[a], John R. Collette[a], and Richard N. Sifers[a,1]

[a]Department of Pathology and Immunology, Baylor College of Medicine, Houston, TX 77030

Edited by Jennifer Lippincott-Schwartz, Janelia Farm Research Campus, Ashburn, VA, and approved August 20, 2020 (received for review October 31, 2019)

The failure of polypeptides to achieve conformational maturation following biosynthesis can result in the formation of protein aggregates capable of disrupting essential cellular functions. In the secretory pathway, misfolded asparagine (N)-linked glycoproteins are selectively sorted for endoplasmic reticulum-associated degradation (ERAD) in response to the catalytic removal of terminal alpha-linked mannose units. Remarkably, ER mannosidase I/Man1b1, the first alpha-mannosidase implicated in this conventional N-glycan-mediated process, can also contribute to ERAD in an unconventional, catalysis-independent manner. To interrogate this functional dichotomy, the intracellular fates of two naturally occurring misfolded N-glycosylated variants of human alpha1-antitrypsin (AAT), Null Hong Kong (NHK), and Z (ATZ), in Man1b1 knockout HEK293T cells were monitored in response to mutated or truncated forms of transfected Man1b1. As expected, the conventional catalytic system requires an intact active site in the Man1b1 luminal domain. In contrast, the unconventional system is under the control of an evolutionarily extended N-terminal cytoplasmic tail. Also, N-glycans attached to misfolded AAT are not required for accelerated degradation mediated by the unconventional system, further demonstrating its catalysis-independent nature. We also established that both systems accelerate the proteasomal degradation of NHK in metabolic pulse-chase labeling studies. Taken together, these results have identified the previously unrecognized regulatory capacity of the Man1b1 cytoplasmic tail and provided insight into the functional dichotomy of Man1b1 as a component in the mammalian proteostasis network.

Man1b1 | mannosidase | ERAD | alpha1-antitrypsin | proteostasis

The survival of multicellular organisms often relies on the capacity of newly synthesized polypeptides to acquire structural maturation within a biologically relevant timeframe (1). However, environmental stress and genetic mutations are sufficient to promote protein misfolding and aggregation in cells (2). Therefore, the capacity of dedicated quality-control systems to identify and promote the intracellular degradation of nonnative polypeptides is crucial for maintaining an optimally functioning cellular status (3). In support of this notion, an imbalance in intracellular protein homeostasis (i.e., proteostasis) is responsible for numerous protein conformational diseases such as cystic fibrosis and alpha1-antitrypsin (AAT) deficiency-related liver disease (4–7).

In the secretory pathway, the opportunistic removal of terminal alpha-linked mannose units functions to "flag" misfolded asparagine (N)-linked glycoproteins as clients for endoplasmic reticulum-associated degradation (ERAD), which designates the pathway that targets misfolded ER proteins for proteasomal degradation (8–12). Mns1p, an alpha-mannosidase in *Saccharomyces cerevisiae*, was the first enzyme identified to contribute to this rate-limiting discriminatory event (13, 14). The human mannosidase ortholog, designated as alpha class 1B member 1 (ER Mannosidase I/Man1b1), belongs to the glycoside hydrolase family 47 (15). It differs from the yeast ortholog by the evolutionary extension of both the cytoplasmic and luminal domains (16). In response to monitoring the intracellular fates of human AAT variants in cell culture, our group introduced the "quality-control timer" model in which the catalysis of terminal alpha-linked mannose by Man1b1 is responsible for promoting misfolded N-glycosylated protein degradation (8, 17). Man1b1 orthologs were originally suggested to catalyze the first mannose trimming step in the processing of mammalian N-linked oligosaccharides and suspected to function in the stepwise process of ERAD client selection (18, 19), but this conclusion has recently been questioned (20).

The human Man1b1 ortholog has been implicated in the pathogenesis of multiple diseases. Pan et al. utilized genetic linkage and functional analyses to identify an association between a single nucleotide polymorphism in the 3′ untranslated region of the human Man1b1 mRNA and infantile end-stage liver disease in patients with alpha1-antitrypsin deficiency (AATD) (21). Defects in Man1b1 have also been linked to a congenital disorder of glycosylation in the form of intellectual disability (22, 23). In addition, Zheng et al. identified that Man1b1 contributes to HIV envelope glycoprotein degradation and implicated a crucial role for the mannosidase in regulating the relative reinfectivity of HIV-1 (24). Moreover, we recently identified that Man1b1 promotes human hepatocellular carcinoma cell survival (25). Finally, an additional group has reported that Man1b1 overexpression is associated with poor prognosis in patients who exhibit bladder cancer (26). Considering the involvement of Man1b1 in the pathogenesis of numerous diseases, plus the aforementioned discrepancy about its catalysis-mediated role in ERAD client selection, a precise understanding of its ERAD client targeting capacity is warranted in order to

Significance

Defects in systems that orchestrate the intracellular clearance of misfolded proteins are implicated as central contributors to numerous human diseases. Our study has further elucidated the unexpected capacity for the prototype mannosidase, Man1b1, to target misfolded alpha1-antitrypsin for intracellular loss by an unconventional, N-glycan-independent manner. Identification of this functional dichotomy, and especially the Man1b1-mediated catalysis-independent system, might influence the design of future therapeutic interventions for selected conformational diseases of the secretory pathway.

Author contributions: A.H.S. and R.N.S. designed research; A.H.S. performed research; A.H.S. analyzed data; and A.H.S., J.R.C., and R.N.S. wrote the paper.

The authors declare no competing interest.

This article is a PNAS Direct Submission.

[1]To whom correspondence may be addressed. Email: rsifers@bcm.edu.

This article contains supporting information online at https://www.pnas.org/lookup/suppl/doi:10.1073/pnas.1919013117/-/DCSupplemental.

First published September 21, 2020.

successfully identify novel therapeutic methods to achieve effective disease management.

To this end, our group reported an unexpected result in which Man1b1 does not require its mannosidase activity or an intact luminal catalytic domain to enhance the ERAD of terminally misfolded AAT variant Null Hong Kong (NHK) (27). In the present study, we further investigated the apparent functional dichotomy of Man1b1 by monitoring the intracellular degradation of two natural ERAD clients, NHK and ATZ. As expected, the capacity of Man1b1 to contribute to the conventional catalysis-dependent ERAD client selection system required an intact active site located in the highly conserved luminal catalytic domain. In contrast, the mannosidase activity was dispensable for the operation of the Man1b1-mediated unconventional system, which was under the control of the evolutionarily extended N-terminal cytoplasmic tail. In addition, the accelerated degradation of terminally misfolded variant NHK was accomplished by either system and both systems can utilize proteasomes to rapidly eliminate NHK. Importantly, Man1b1's participation in the unconventional system did not require N-glycans attached to either of the client proteins. Based on these data, we propose a model in which the evolutionary elongation of the cytoplasmic tail provides an unexpected level of functional plasticity for Man1b1, thereby expanding the capacity of the proteostasis network in the mammalian secretory pathway. A potential role for the extended Man1b1 cytoplasmic tail is discussed.

Results

Elimination of the Man1b1 Cytoplasmic Tail Leads to Intracellular Accumulation of Misfolded AAT Proteins. The human Man1b1 protein consists of 699 amino acids and includes an N-terminal cytoplasmic tail, a transmembrane domain, and a C-terminal

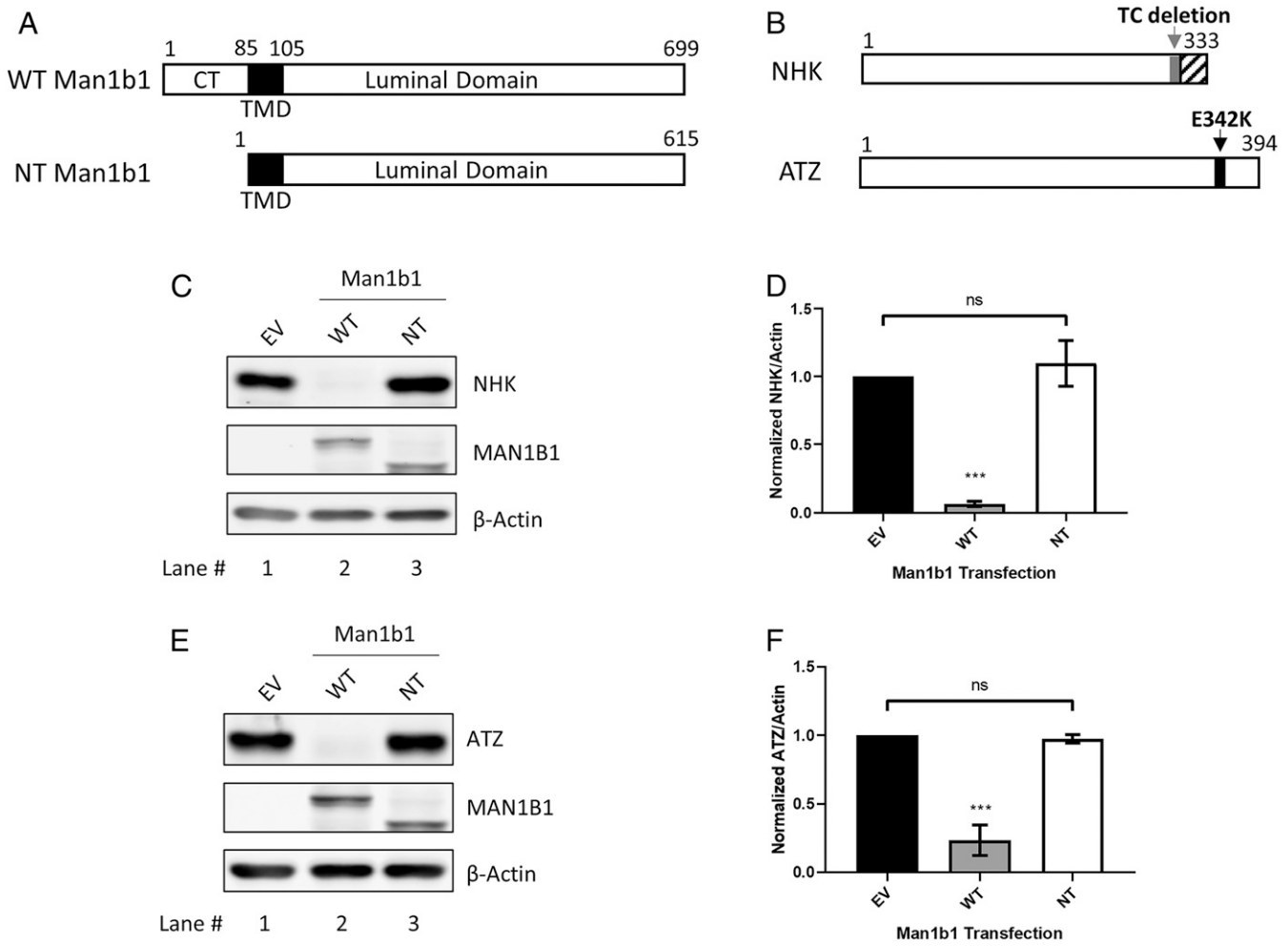

Fig. 1. The cytoplasmic tail of human Man1b1 is essential for promoting misfolded AAT elimination under steady-state conditions. (*A*) Schematic of WT and no-tail (NT) human Man1b1 proteins. Man1b1 consists of an N-terminal cytoplasmic tail (CT), a transmembrane domain (TMD), and a C-terminal luminal domain. NT Man1b1 was generated by site-directed mutagenesis to remove the entire cytoplasmic tail. (*B*) Schematic of two misfolded AAT variants, NHK and ATZ. NHK has an early stop codon caused by deletion of a TC dinucleotide. ATZ has the single E342K mutation. (*C*) Steady-state whole cell lysate Western blots of 293T E7 (Man1b1-KO) cells transfected with NHK and constructs encoding empty vector (EV), WT, or NT Man1b1. Cells were lysed 24 h posttransfection. Lysates were resolved by 10% SDS/PAGE. Western blots shown are representative of four independent experiments. (*D*) Graphic representations of NHK levels normalized to actin in whole cell lysates from the steady-state Western blot experiments shown in *C*. Data are reported as the mean ± SEM with statistical significance calculated by one-way ANOVA and Tukey's multiple comparisons test. ns, not significant. $***P \leq 0.001$, $n = 4$. (*E*) Steady-state whole cell lysate Western blot of 293T E7 cells transfected with ATZ and constructs encoding EV, WT, or NT Man1b1. Western blots shown are representative of three independent experiments. (*F*) Graphic representations of ATZ levels normalized to actin in whole cell lysates from the steady-state Western blot experiments shown in *E*. Data are reported as the mean ± SEM with statistical significance calculated by one-way ANOVA and Tukey's multiple comparisons test. ns, not significant. $***P \leq 0.001$, $n = 3$.

luminal tail that contains the catalytic domain (Fig. 1*A*). We previously reported that Man1b1 contributes to the accelerated proteasomal degradation of two misfolded asparagine (N)-glycosylated ERAD clients, designated NHK and ATZ, both of which are natural genetic variants of alpha1-antitrypsin (AAT) (17, 27–29). NHK is a terminally misfolded AAT variant that exhibits an early stop codon caused by a dinucleotide (TC) deletion (28) (Fig. 1*B*). In contrast, ATZ is a secretion-impaired variant in which the glutamate 342 to lysine mutation (E342K) generates a kinetic folding trap that impairs conformational maturation of the polypeptide (30–33) (Fig. 1*B*). Since its discovery (28), NHK has arguably served as the most highly studied ERAD client (34–37), and ATZ has been linked to the development of liver disease (6, 38).

Herein, we utilized transient transfection to examine the capacity of the Man1b1 cytoplasmic tail to influence the degradation of NHK and ATZ in 293T E7 cells where CRISPR/Cas9 technology had eliminated the expression of endogenous Man1b1 (24). We first generated "no-tail (NT)" Man1b1 by removing the entire N-terminal cytoplasmic tail of human Man1b1 without altering any of the additional domains by site-directed mutagenesis (Fig. 1*A*). In our initial studies, experiments were performed under steady-state conditions to provide us with a simple and rapid screening method. As demonstrated in other cell types (17, 27), wild-type (WT) Man1b1 significantly enhanced the intracellular loss of NHK as compared to NHK plus empty vector (EV) (Fig. 1*C*, lanes 1 and 2, and Fig. 1*D*). In contrast, NT Man1b1 failed to enhance NHK intracellular loss as

A

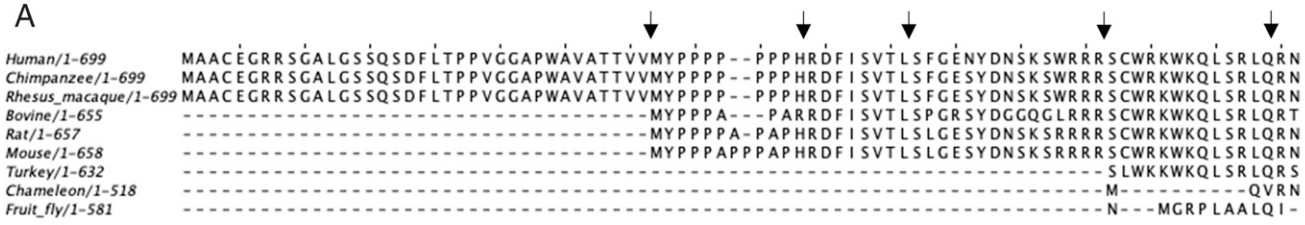

B

Man1b1	Sequence (amino acids)
WT	MAACEGRRSGALGSSQSDFLTPPVGGAPWAVATTVVMYPPPPPPPHRDFISVTLSFGESYDNSKSWRRRSCWRKWKQLSRLQRN
Δ1-36	MYPPPPPPPHRDFISVTLSFGESYDNSKSWRRRSCWRKWKQLSRLQRN
Δ1-46	MRDFISVTLSFGESYDNSKSWRRRSCWRKWKQLSRLQRN
Δ1-54	MSFGESYDNSKSWRRRSCWRKWKQLSRLQRN
Δ1-69	MSCWRKWKQLSRLQRN
Δ1-82	MRN

C

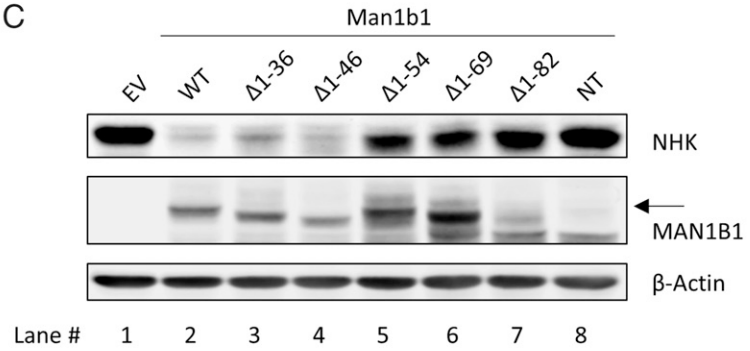

D

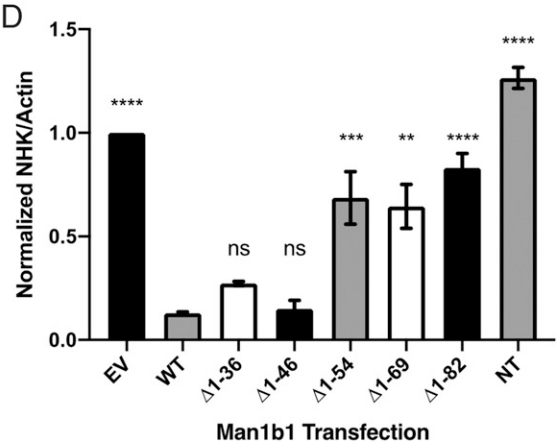

Fig. 2. Sequential N-terminal truncations of the cytoplasmic tail impair Man1b1's capacity in promoting NHK elimination under steady-state conditions. (*A*) Multiple amino acid sequence alignments of the Man1b1 cytoplasmic tails across lower and higher organisms using Jalview software. Five black arrows indicate the truncation sites for different human Man1b1 constructs used in the experiments that follow. (*B*) List of truncated Man1b1 expression constructs used in the subsequent experiments. (*C*) Steady-state whole cell lysate Western blots of 293T E7 cells transfected with NHK and constructs encoding EV, WT, Δ1 to 36, Δ1 to 46, Δ1 to 54, Δ1 to 69, Δ1 to 82, or NT Man1b1. Western blots shown are representative of three independent experiments. The black arrow indicates O-glycosylated Man1b1 discussed in Fig. 7. (*D*) Graphic representations of NHK levels normalized to actin in whole cell lysates from the steady-state Western blot experiments shown in *C*. Data are reported as the mean ± SEM with statistical significance calculated by one-way ANOVA and Tukey's multiple comparisons test. ns, not significant. $^{**}P \leq 0.01$, $^{***}P \leq 0.001$, $^{****}P \leq 0.0001$, $n = 3$.

observed for WT Man1b1 (Fig. 1*C*, lanes 2 and 3, and Fig. 1*D*). Likewise, in a parallel set of experiments, similar results were observed for ATZ (Fig. 1 *E* and *F*). In summary, the cytoplasmic tail of Man1b1 is required to accelerate the intracellular loss of misfolded AAT variants measured under steady-state conditions.

Sequential Man1b1 Cytoplasmic Tail Truncations Gradually Impair the Enhancement of NHK Intracellular Loss. To further examine the regulatory capacity of the cytoplasmic tail to accelerate misfolded AAT degradation, we performed an amino acid sequence alignment of the cytoplasmic tails for several Man1b1 orthologs (Fig. 2*A*). The analysis revealed that the cytoplasmic tail had undergone significant elongation during the course of evolution. Thus, we hypothesized that the addition of amino acids to human Man1b1 could have endowed the cytoplasmic tail with a novel regulatory capacity in terms of promoting the use of an alternative ERAD client recruitment system.

To test this hypothesis, a series of N-terminal truncations were generated based on the comparative sequence alignment, and these were designated as Δ1 to 36, Δ1 to 69, and Δ1 to 82 Man1b1 (Fig. 2*B*). Next, we cotransfected 293T E7 cells with NHK and various Man1b1 expression plasmids including WT, Δ1 to 36, Δ1 to 69, Δ1 to 82, NT Man1b1, and empty vector, respectively. Whole cell lysates were generated 24 h post-transfection and the levels of intracellular NHK were compared by Western blotting following sodium dodecyl sulfate polyacrylamide gel electrophoresis (SDS/PAGE). Enhanced intracellular loss of NHK was observed in response to expression of either WT or Δ1 to 36 Man1b1 (Fig. 2*C*, lanes 1 to 3, and Fig. 2*D*). However, removal of larger segments of the cytoplasmic tail (Δ1 to 69 and Δ1 to 82) gradually hindered this trend for NHK (Fig. 2*C*, lanes 1, 2, 6, and 7, and Fig. 2*D*). To further investigate the differential effect of Δ1 to 36 and Δ1 to 69 Man1b1 on NHK fate, two additional Man1b1 truncations, Δ1 to 46 and Δ1 to 54, were generated in response to the protein prediction algorithm of functional effects of mutations (predictprotein.org) (*SI Appendix*, Fig. S1). Importantly, Δ1 to 46 Man1b1 promoted the intracellular loss of NHK to a similar extent as both WT and Δ1 to 36 Man1b1 (Fig. 2*C*, lanes 1 to 4, and Fig. 2*D*). However, cotransfected Δ1 to 54 Man1b1 hindered NHK elimination in a pattern that was similar to that of Δ1 to 69 Man1b1 (Fig. 2*C*, lanes 5 and 6, and Fig. 2*D*).

Amino Acids 1 to 54 of Man1b1 Are Essential to Accelerate ATZ Degradation. After identifying the capacity of Δ1 to 54 Man1b1 to hinder, but not entirely ablate, the loss of NHK, we examined its effect on the fate of ATZ. Importantly, Δ1 to 54 Man1b1 entirely disrupted the accelerated intracellular loss of ATZ as compared to the capacity of WT Man1b1 at steady state (Fig. 3 *A* and *B*). To gain a greater understanding about this dynamic process, we utilized ^{35}S metabolic pulse-chase radiolabeling to monitor the fate of newly synthesized ATZ in 293T E7 cells in the presence of the empty vector, WT Man1b1 or Δ1 to 54 Man1b1. Immunoprecipitation from the cell lysates was performed with a polyclonal antibody against AAT to isolate ATZ, and the relative signal intensity was quantified following SDS/PAGE. The influence on intracellular ATZ levels over a 5-h chase is shown in Fig. 3*C*, and the quantified results from three independent experiments are plotted in Fig. 3*D*. Over the course of 5 h, detection of the pulse-radiolabeled ATZ cohort gradually decreased in the absence of transfected Man1b1, which was likely due to compensation by other protein quality-control pathways. As expected, transfected WT Man1b1 significantly accelerated the disappearance of pulse-radiolabeled ATZ at 1-h and 3-h timepoints (Fig. 3*D*). Importantly, consistent with our prior steady-state Western blot analyses (Fig. 3 *A* and *B*), transfection with Δ1 to 54 Man1b1 failed to accelerate the intracellular loss of ATZ (Fig. 3 *C* and *D*). In summary, both steady-state analyses and radioactive pulse-chase experiments demonstrated that amino acids 1 to 54 of the Man1b1 cytoplasmic tail are required to accelerate the Man1b1-mediated loss of ATZ in 293T E7 cells. Hereafter, we refer to the cytoplasmic tail-dependent acceleration of misfolded protein loss as the unconventional Man1b1-mediated system.

Operation of the Unconventional Man1b1-Mediated System Is Independent of N-Glycan Trimming. Man1b1 is traditionally categorized as one of many alpha-mannosidases belonging to the glycoside hydrolase family 47 (15, 16). Its catalytic domain exists within a large C-terminal luminal domain. Previous research has established the ability of the catalytic domain to catalyze the hydrolysis of one or more terminal mannose units from N-linked glycosylated protein substrates (39–41). Here we raised the question whether the newly discovered unconventional function of Man1b1 is independent of its catalytic function. To explore the relationship between the conventional catalysis-dependent system of Man1b1 and the unconventional cytoplasmic tail-dependent system, Man1b1 expression constructs were generated in which one of the two functional domains was ablated by site-directed mutagenesis. Specifically, we generated the catalytic-dead Man1b1 with the D463N mutation in the catalytic domain, which was previously reported to diminish 99.9% of the inherent catalytic activity of human Man1b1 (41) (Fig. 4*A*). The second construct, Δ1 to 54 Man1b1, was characterized earlier as the cytoplasmic tail-truncated form that contained an intact catalytic domain (Fig. 2). The third construct contained both modifications and was designated as Δ1 to 54 D463N Man1b1.

WT, D463N, Δ1 to 54, and Δ1 to 54 D463N Man1b1 were coexpressed with NHK in 293T E7 cells. The catalytic-dead (D463N) and the cytoplasmic tail-truncated (Δ1 to 54) Man1b1 both partially hindered NHK loss when compared to the accelerated loss caused by WT Man1b1 (Fig. 4*B*, lanes 1 to 4). Specifically, WT Man1b1 promoted 90% NHK disappearance as compared to EV, D463N Man1b1 promoted 82%, and Δ1 to 54 Man1b1 promoted 60% (Fig. 4*C*). In contrast, Δ1 to 54 D463N Man1b1 promoted only a 27% NHK disappearance and presented an additive effect in enhancing NHK loss (Fig. 4*B*, lane 5, and Fig. 4*C*). The quantification of five independent experiments (Fig. 4*C*) supported a model in which the accelerated intracellular loss of NHK was promoted by both the conventional catalytic and the unconventional cytoplasmic tail-dependent systems. This additive effect seen in Δ1 to 54 D463N Man1b1 provided evidence that the unconventional system operates independently of the catalytic function.

Considering our observation that the deletion of amino acids 1 to 54 from Man1b1 completely abolished its capacity to accelerate ATZ degradation (Fig. 3), we repeated the preceding experiments with ATZ as the client. Cotransfection with either WT or catalytic-dead Man1b1 (D463N) significantly accelerated the loss of ATZ from cell lysates by 82% and 74%, respectively, compared to EV (Fig. 4*D*, lanes 1 to 3, and Fig. 4*E*). Δ1 to 54 Man1b1 did not significantly accelerate ATZ loss compared to EV, which agrees with the results shown in Fig. 3. It is worth noting that we observed hindered electrophoretic mobility of ATZ in response to cotransfection with D463N Man1b1 (Fig. 4 *D*, *Top*, compare lanes 1 to 3), confirming that the D463N mutation had abrogated N-glycan trimming. By contrast, the electrophoretic mobility of ATZ in the Δ1 to 54 Man1b1 group implies efficient trimming (Fig. 4 *D*, *Top*, compare lanes 1 to 4), suggesting the presence of the catalytic function in Δ1 to 54 Man1b1. Taken together, these observations imply that post-translational N-glycan modification was dispensable for accelerating the loss of ATZ by Man1b1. This conclusion was further substantiated by the inability of Δ1 to 54 D463N Man1b1 to influence ATZ fate or enhance glycan-mediated changes in electrophoretic mobility in SDS/PAGE (Fig. 4*D*, lane 5, and

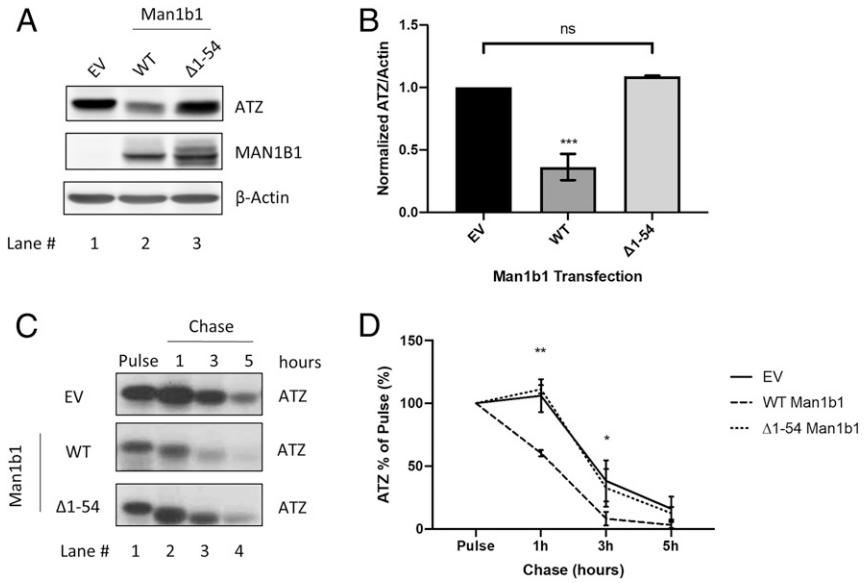

Fig. 3. Amino acids 1 to 54 of Man1b1 are required to accelerate ATZ degradation. (*A*) Steady-state whole cell lysate Western blots of 293T E7 cells transfected with ATZ and constructs encoding EV, WT, or Δ1 to 54 Man1b1. Western blots shown are representative of three independent experiments. (*B*) Graphic representations of ATZ levels normalized to actin in whole cell lysates from the steady-state Western blot experiments shown in *A*. Data are reported as the mean ± SEM with statistical significance calculated by one-way ANOVA and Tukey's multiple comparisons test. ns, not significant. $***P \leq 0.001$, $n = 3$. (*C*) ^{35}S metabolic pulse-chase radiolabeling analyses of 293T E7 cells transfected with ATZ and constructs encoding EV, WT, or Δ1 to 54 Man1b1. At 24 h posttransfection, cells were labeled for 15 min with [^{35}S]methionine and [^{35}S]cysteine, then chased at 1 h, 3 h, and 5 h. The gels shown are representative of three independent experiments. (*D*) Graphic representations of ATZ levels in pulse-chase experiments shown in *C*. Data are reported as the mean ± SEM with statistical significance calculated by two-way ANOVA and Tukey's multiple comparisons test. ns, not significant. $*P \leq 0.05$, $**P \leq 0.01$, $n = 3$.

Fig. 4*E*). Finally, to rule out the possibility that the observed pattern in intracellular NHK and ATZ levels shown in Fig. 4 was due to protein secretion, the AAT concentrations in the cell culture media were examined. Only a miniscule amount of NHK was detected in the cell media (*SI Appendix*, Fig. S2*A*). Although some levels of ATZ were detected, it was far less abundant than the intracellular cohort and exhibited the same concentration pattern as in Fig. 4*D* (*SI Appendix*, Fig. S2*B*). In summary, these data indicated that the unconventional Man1b1 cytoplasmic tail-mediated pathway functions independently of the conventional catalytic function of Man1b1 in accelerating the intracellular loss of misfolded AAT.

N-Glycans Are Dispensable for Accelerating AAT Disappearance by the Unconventional Man1b1-Mediated System. To further investigate the apparent domain-specific dichotomy in which Man1b1 can promote AAT intracellular loss through the use of distinct systems, we decided to examine the consequences of eliminating N-glycans on the misfolded AAT clients. We hypothesized that N-glycans are dispensable for the unconventional system of Man1b1 because of its catalysis-independent manner demonstrated above (Fig. 4). To test this hypothesis, we first took advantage of the previously established NHK mutant, NHK-QQQ (27, 42) in which the three asparagine residues (N46, N83, and N247) for N-glycans are mutated to glutamines to prevent N-glycosylation (Fig. 5*A*).

In an identical experimental setting as described in Fig. 4*B*, 293T E7 cells were coexpressed with NHK-QQQ plus one of the four different forms of Man1b1, namely, WT, D463N, Δ1 to 54, and Δ1 to 54 D463N. In support of our hypothesis, the effects on intracellular NHK-QQQ levels were distinct from that of N-glycosylated NHK (compare Fig. 5 *B* and *C* and Fig. 4 *B* and *C*). First, no differences were detected in the levels of NHK-QQQ in cells coexpressing WT Man1b1 or D463N Man1b1 (Fig. 5*B*, lanes 1 to 3, and Fig. 5*C*). This was expected because WT Man1b1 cannot exert the catalytic function to promote the degradation of non-N-glycosylated protein clients. Similarly, Δ1 to 54 and Δ1 to 54 D463N Man1b1 exhibited no significant difference in promoting NHK-QQQ loss (Fig. 5*B*, lanes 1, 4, and 5, and Fig. 5*C*). More importantly, the removal of amino acids 1 to 54 from Man1b1 completely ablated the accelerated loss of intracellular NHK-QQQ (Fig. 5*B*, lanes 1 and 4, and Fig. 5*C*). Collectively the results suggest, first, the entire population of NHK-QQQ is subjected to the unconventional Man1b1 cytoplasmic tail-mediated pathway; second, this cytoplasmic tail-mediated system operates independently from the glycosylation status of the misfolded protein clients. Importantly, these observations are in agreement with our conclusion that the unconventional Man1b1 cytoplasmic tail-mediated system operates in an N-glycan catalysis-independent manner (Fig. 4).

To further validate our conclusions, we next generated a non-N-glycosylated form of ATZ, namely ATZ-QQQ (Fig. 5*A*), and performed a set of experiments identical to those described above for NHK-QQQ. The detected pattern of ATZ-QQQ protein levels was identical to that of NHK-QQQ, and the removal of amino acids 1 to 54 completely ablated the capacity of Man1b1 to accelerate ATZ-QQQ disappearance (Fig. 5 *D* and *E*). Again, these results further confirmed the functional independence that exists between the catalytic activity and the unconventional cytoplasmic tail-mediated system, providing functional plasticity of Man1b1 in promoting misfolded protein elimination.

Proteasomal Degradation can Contribute to the Conventional and Unconventional Intracellular Elimination of NHK. In the present study, steady-state conditions were utilized as the primary means to compare and contrast the capacity of Man1b1's luminal catalytic domain and cytoplasmic tail in altering the fate of misfolded protein clients. To validate our findings, we performed ^{35}S metabolic pulse-chase radiolabeling in the presence of a

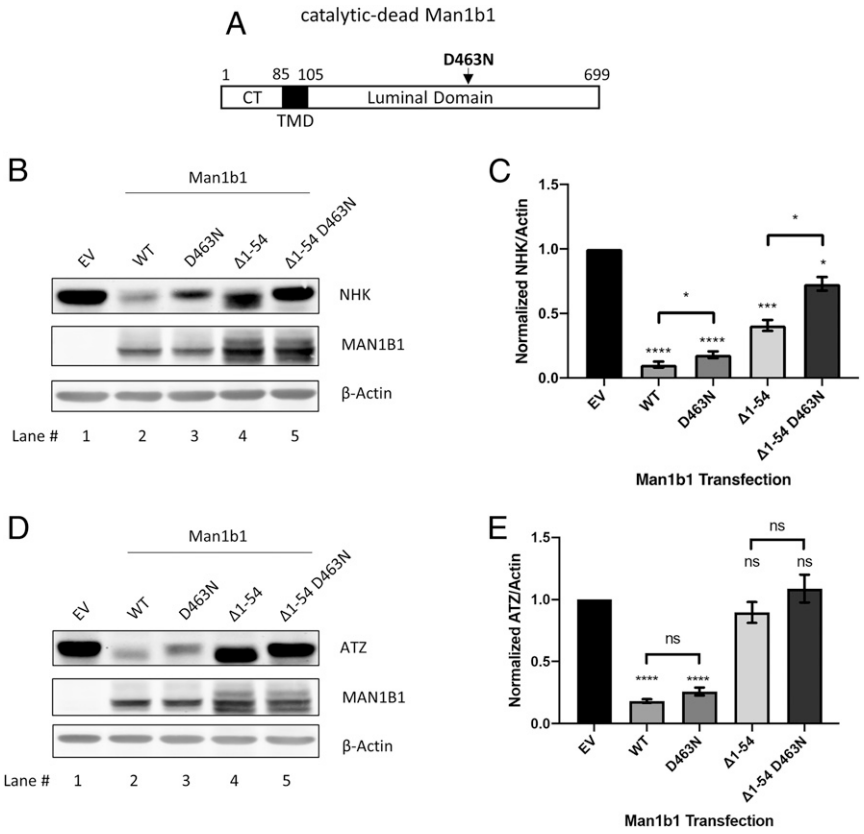

Fig. 4. Man1b1 cytoplasmic tail-mediated elimination of misfolded AAT is independent of Man1b1's catalytic function. (*A*) Schematic of the catalytic-dead Man1b1 protein with the indicated amino acid mutation D463N. (*B*) Steady-state whole cell lysate Western blots of 293T E7 cells transfected with NHK and constructs encoding EV, WT, D463N, Δ1 to 54, or Δ1 to 54 D463N Man1b1. Western blots shown are representative of five independent experiments. (*C*) Graphic representations of NHK levels normalized to actin in whole cell lysates from the steady-state Western blot experiments shown in *B*. Data are reported as the mean ± SEM with statistical significance calculated by one-way ANOVA and Tukey's multiple comparisons test. $*P \leq 0.05$, $***P \leq 0.001$, $****P \leq 0.0001$, $n = 5$. (*D*) Steady-state whole cell lysate Western blots of 293T E7 cells transfected with ATZ and constructs encoding EV, WT, D463N, Δ1 to 54, or Δ1 to 54 D463N Man1b1. Western blots shown are representative of five independent experiments. (*E*) Graphic representations of ATZ levels normalized to actin in whole cell lysates from the steady-state Western blot experiments shown in *D*. Data are reported as the mean ± SEM with statistical significance calculated by one-way ANOVA and Tukey's multiple comparisons test. ns, not significant. $****P \leq 0.0001$, $n = 5$.

proteasomal (lactacystin) or lysosomal inhibitor (bafilomycin) to identify which, if either, proteolytic system was responsible for Man1b1-mediated intracellular elimination of misfolded proteins. We first chose NHK as the client in this study because its fate was influenced by both the conventional catalytic system and the unconventional cytoplasmic tail-mediated system under steady-state conditions (Fig. 4 *B* and *C*). This characteristic makes NHK an ideal candidate to differentially study the two apparent functions of Man1b1 with respect to the promotion of misfolded protein degradation. We coexpressed NHK with WT Man1b1 in 293T E7 cells then treated cells with dimethyl sulfoxide (DMSO), lactacystin, or bafilomycin for 12 h. ^{35}S metabolic pulse-chase radiolabeling results revealed that proteasomal inhibition by lactacystin delayed Man1b1-mediated NHK degradation while lysosomal inhibition by bafilomycin exerted no significant effect (Fig. 6 *A*–*C*). To separate the conventional catalysis-dependent system and the unconventional cytoplasmic tail-mediated system, we next cotransfected 293T E7 cells with either NHK and Δ1 to 54 Man1b1 (Fig. 6 *D*–*F*), or NHK and D463N Man1b1 (Fig. 6 *G*–*I*). As compared to the DMSO negative control group, lactacystin treatment significantly inhibited the intracellular degradation of NHK at the 3-h timepoint in cells cotransfected with Δ1 to 54 Man1b1 (Fig. 6 *D* and *E*). In contrast, bafilomycin treatment did not significantly impact NHK disposal (Fig. 6*F*), although the 12-h treatment sufficiently induced increased levels of LC3B-II (*SI Appendix*, Fig. S3) as validation for the inhibitory capacity of bafilomycin under our experimental conditions. These results suggest that the conventional Man1b1 catalysis-dependent NHK degradation utilizes active proteasomes. In a parallel set of experiments using D463N Man1b1, we observed that lactacystin treatment, but not bafilomycin treatment, significantly delayed NHK degradation at 1-h and 3-h timepoints (Fig. 6 *G*–*I*). Based on these results, we conclude that proteasomal degradation functions as the common endpoint for the conventional and unconventional intracellular degradation of NHK promoted by Man1b1. Unexpectedly, in a parallel setup using ATZ as the client, we observed that the influence of WT, Δ1 to 54, and D463N Man1b1 on ATZ degradation appeared refractory to inhibitors of both proteasomal and lysosomal degradation (*SI Appendix*, Fig. S4).

In addition, we further analyzed the aforementioned results by comparing NHK degradation trends in the DMSO vehicle control groups from the WT, D463N, and Δ1–54 Man1b1 samples (Fig. 6*J*). The comparative analysis further confirmed our observation from the steady-state experiments that Δ1 to 54 Man1b1 significantly delayed NHK degradation compared to WT Man1b1 (Figs. 2 *C* and *D* and 4 *B* and *C*). Although the difference of NHK degradation rates between WT and D463N Man1b1 groups did not reach statistical significance, D463N Man1b1 delayed NHK degradation at all timepoints on average in three independent experiments (Fig. 6*J*), which possibly explains why the difference is only minimal under steady-state

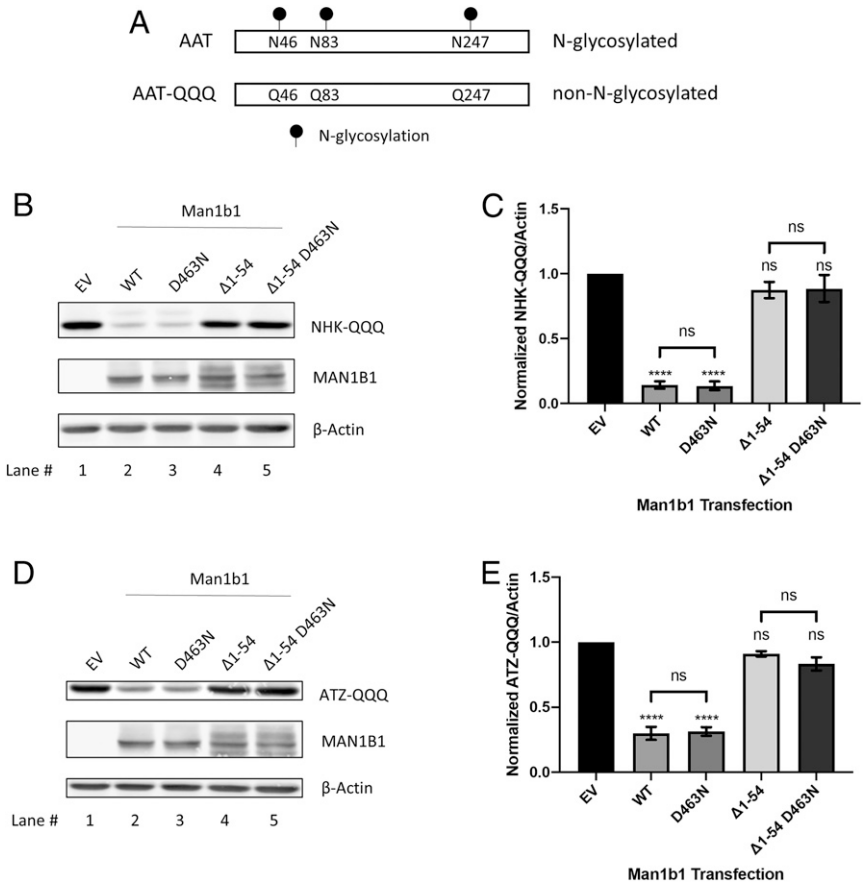

Fig. 5. Man1b1 cytoplasmic tail-mediated elimination of misfolded AAT is independent of AAT glycosylation status. (*A*) Schematic of N-glycosylated AAT versus nonglycosylated AAT-QQQ harboring N46Q, N83Q, and N247Q mutations. (*B*) Steady-state whole cell lysate Western blots of 293T E7 cells transfected with NHK-QQQ and constructs encoding EV, WT, D463N, Δ1 to 54, or Δ1 to 54 D463N Man1b1. Western blots shown are representative of three independent experiments. (*C*) Graphic representations of NHK-QQQ levels normalized to actin in whole cell lysates from the steady-state Western blot experiments shown in *B*. Data are reported as the mean ± SEM with statistical significance calculated by one-way ANOVA and Tukey's multiple comparisons test. ns, not significant. ****$P \leq 0.0001$, $n = 3$. (*D*) Steady-state whole cell lysate Western blots of 293T E7 cells transfected with ATZ-QQQ and constructs encoding EV, WT, D463N, Δ1 to 54, or Δ1 to 54 D463N Man1b1. Western blots shown are representative of three independent experiments. (*E*) Graphic representations of ATZ-QQQ levels normalized to actin in whole cell lysates from the steady-state Western blot experiments shown in *D*. Data are reported as the mean ± SEM with statistical significance calculated by one-way ANOVA and Tukey's multiple comparisons test. ns, not significant. ****$P \leq 0.0001$, $n = 3$.

conditions (Fig. 4*B* compare lanes 2 and 3, Fig. 4*C* compare columns 2 and 3).

Δ1 to 54 Man1b1 Is Subjected to O-Linked Glycosylation. In addition to the functional differences of how WT and Δ1 to 54 Man1b1 accelerate misfolded AAT degradation, we also observed a unique banding pattern for Δ1 to 54 Man1b1. Specifically, a ladder of immunoreactive bands was detected by Western blotting that migrated more slowly than the predicted size, particularly for Δ1 to 54 and Δ1 to 69 Man1b1 (Fig. 2*C*, black arrow). The unique electrophoretic pattern was reminiscent of Man1b1 O-linked glycosylation discovered by our group previously as biochemical evidence that Man1b1 is a resident enzyme of the Golgi complex (43). In the prior study, O-linked glycans bearing terminal sialic acid units, as a type of Golgi-situated posttranslational modification, were identified on threonine (Thr)-186, Thr-204, Thr-230, and Thr-239 residues of endogenous Man1b1 expressed in HeLa cells (43). However, in 293T E7 cells used as the host in the present study, O-glycosylated bands for WT Man1b1 were rarely detected, implying that the extent of O-glycosylation likely substantially varies between cell lines. To determine whether the ladder of bands detected for Δ1 to 54 Man1b1 reflects O-glycosylation, the corresponding transfected cell lysates were incubated with Sialidase A to catalyze the in vitro removal of terminal sialic acids, and then analyzed by Western blotting. Incubation with Sialidase A increased the electrophoretic mobility of the upper bands compared to the mock incubation (Fig. 7*A*, lanes 7 and 8), confirming the ladder of immunoreactive bands had been caused by intracellular sialic acid-containing modifications. To validate the specific O-glycosylation sites, all four of the previously identified O-glycosylated threonine residues were mutated to alanine in both WT and Δ1 to 54 Man1b1, designated as O-deficient (O-def) Man1b1 (Fig. 7*B*). Subsequently, a combination of transient transfection and Western blotting of cell lysates identified only a single immunoreactive band, rather than a ladder of glycosylated forms (Fig. 7*C*). These data provide solid evidence that Δ1 to 54 Man1b1 selectively undergoes O-glycosylation when expressed in 293T E7 cells.

To investigate whether O-glycosylation is responsible for the observed hindrance of ERAD client degradation by Δ1 to 54 Man1b1, 293T E7 cells were cotransfected with ATZ and O-def Man1b1, and the relative intracellular ATZ concentrations were determined 24 h posttransfection. The Western blot results in Fig. 7*D* and quantification in Fig. 7*E* show that the absence of Δ1 to 54 Man1b1 O-glycosylation did not rescue the degradation of

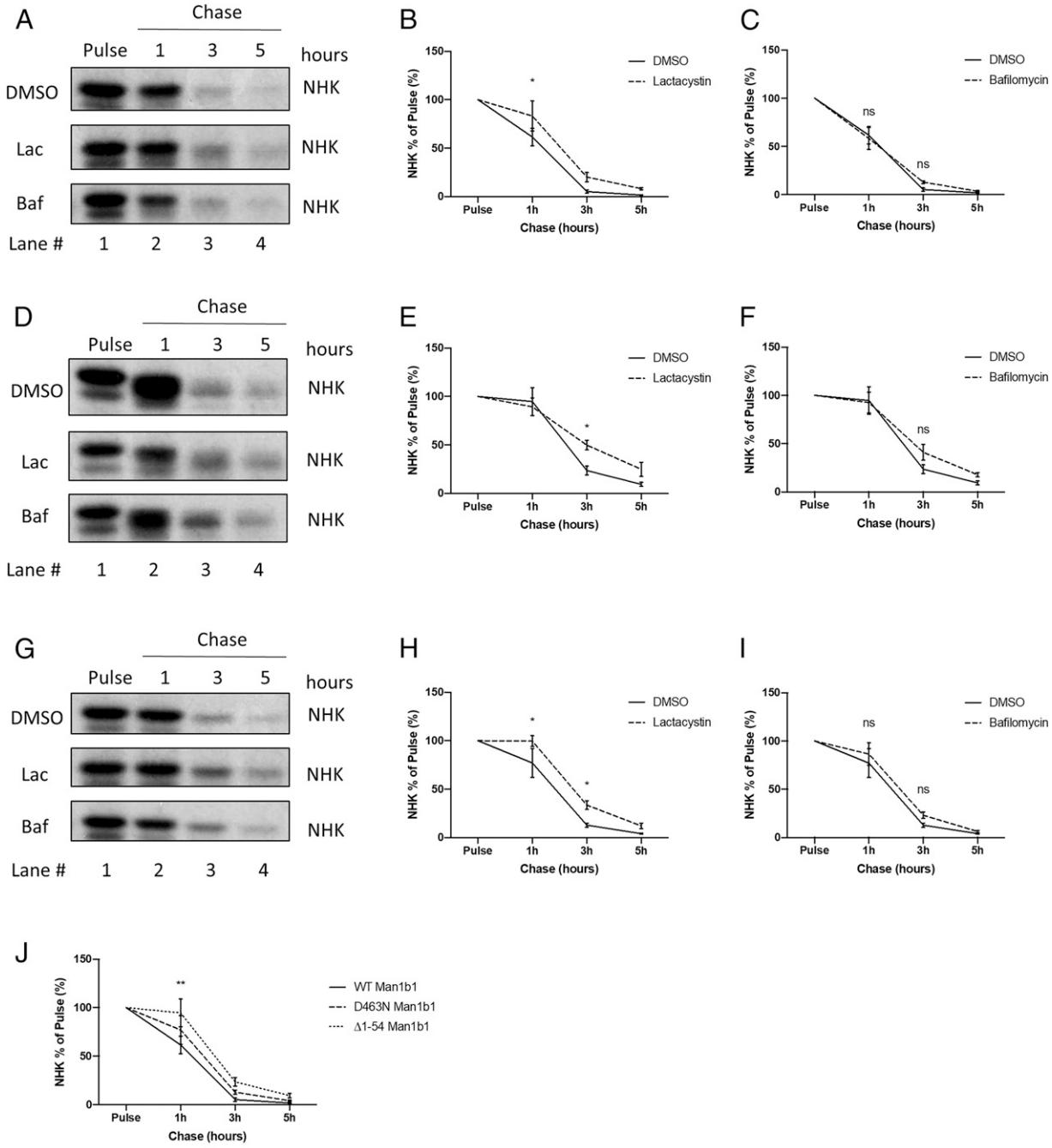

Fig. 6. Proteasomal degradation functions as a common endpoint for the conventional and unconventional intracellular degradation of NHK promoted by Man1b1. (*A*) ^{35}S metabolic pulse-chase radiolabeling analyses of 293T E7 cells transfected with NHK and WT Man1b1 constructs. At 12 h posttransfection, cells were treated with DMSO, lactacystin, or bafilomycin for 12 h. Cells were then labeled for 15 min with [^{35}S]methionine and [^{35}S]cysteine, then chased at 1 h, 3 h, and 5 h with the same inhibitor treatments present in the media. The gels shown are representative of three independent experiments. (*B* and *C*) Graphic representations of NHK levels in pulse-chase experiments shown in *A*. Data are reported as the mean ± SEM with statistical significance calculated by two-way ANOVA and Dunnett's multiple comparisons test. ns, not significant. $*P \leq 0.05$, $n = 3$. (*B*) Comparison between DMSO and lactacystin groups from *A*. (*C*) Comparison between DMSO and bafilomycin groups from *A*. (*D*) ^{35}S metabolic pulse-chase radiolabeling analyses of 293T E7 cells transfected with NHK and Δ1 to 54 Man1b1 constructs in a parallel setting as shown in *A*. (*E* and *F*) Graphic representations of NHK levels in pulse-chase experiments shown in *D*. Data are reported as the mean ± SEM with statistical significance calculated by two-way ANOVA and Dunnett's multiple comparisons test. ns, not significant. $*P \leq 0.05$, $n = 3$. (*E*) Comparison between DMSO and lactacystin groups from *D*. (*F*) Comparison between DMSO and bafilomycin groups from *D*. (*G*) ^{35}S metabolic pulse-chase radiolabeling analyses of 293T E7 cells transfected with NHK and D463N Man1b1 constructs in a parallel setting as shown in *A*. (*H* and *I*) Graphic representations of NHK levels in pulse-chase experiments shown in *G*. Data are reported as the mean ± SEM with statistical significance calculated by two-way ANOVA and Dunnett's multiple comparisons test. ns, not significant. $*P \leq 0.05$, $n = 3$. (*H*) Comparison between DMSO and lactacystin groups from *G*. (*I*) Comparison between DMSO and bafilomycin groups from *G*. (*J*) Graphic representations of NHK levels in DMSO-treated samples from the ^{35}S metabolic pulse-chase experiments shown in *A*, *D*, and *G*. Data are reported as the mean ± SEM with statistical significance calculated by two-way ANOVA and Tukey's multiple comparisons test. $**P \leq 0.01$ (between WT and Δ1 to 54 Man1b1 samples at 1-h timepoint), $n = 3$.

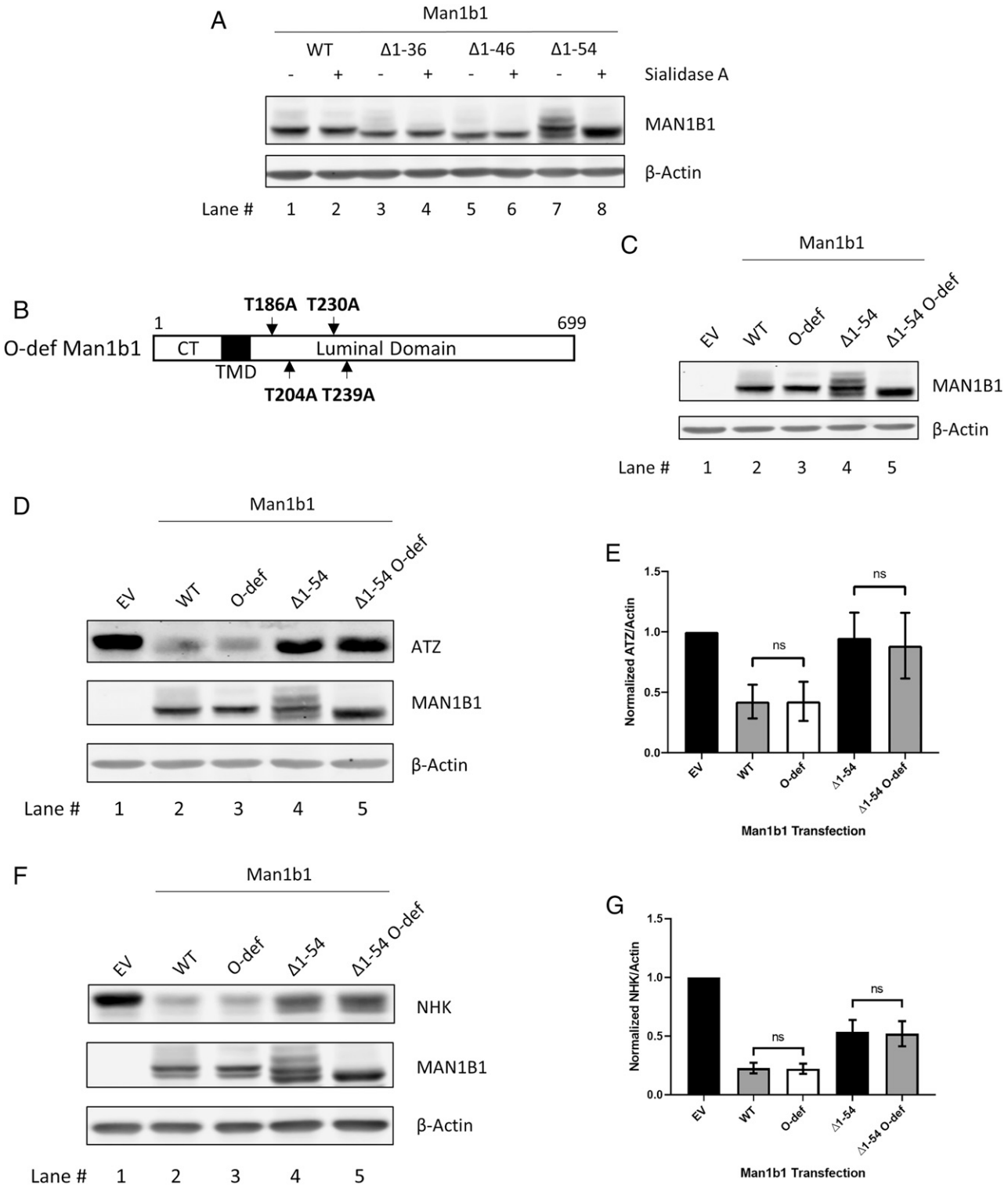

Fig. 7. Δ1 to 54 Man1b1 is subjected to O-linked glycosylation. (*A*) Steady-state whole cell lysate Western blots of 293T E7 cells transfected with constructs encoding WT, Δ1 to 36, Δ1 to 46, or Δ1 to 54 Man1b1. Lysates were treated with Sialidase A (+) or mock-treated (–) for 1 h at 37 °C. (*B*) Schematic of O-deficient (O-def) Man1b1 protein with the four previously discovered O-glycosylation sites mutated from threonine to alanine. (*C*) Steady-state whole cell lysate Western blots of 293T E7 cells transfected with constructs encoding EV, WT, O-def, Δ1 to 54, or Δ1 to 54 O-def Man1b1. (*D*) Steady-state whole cell lysate Western blots of 293T E7 cells transfected with ATZ and constructs encoding EV, WT, O-def, Δ1 to 54, or Δ1 to 54 O-def Man1b1. Western blots shown are representative of three independent experiments. (*E*) Graphic representations of ATZ levels normalized to actin in whole cell lysates from the steady-state Western blot experiments shown in *D*. Data are reported as the mean ± SEM with statistical significance calculated by one-way ANOVA and Tukey's multiple comparisons test. ns, not significant, $n = 3$. (*F*) Steady-state whole cell lysate Western blots of 293T E7 cells transfected with NHK and constructs encoding EV, WT, O-def, Δ1 to 54, or Δ1 to 54 O-def Man1b1. Western blots shown are representative of three independent experiments. (*G*) Graphic representations of NHK levels normalized to actin in whole cell lysates from the steady-state Western blot experiments shown in *F*. Data are reported as the mean ± SEM with statistical significance calculated by one-way ANOVA and Tukey's multiple comparisons test. ns, not significant, $n = 3$.

ATZ (Fig. 7 *D* and *E*). In a parallel set of experiments using NHK as the client, we obtained similar results where the expression of Δ1 to 54 and Δ1 to 54 O-def Man1b1 did not exhibit a differential effect on NHK degradation (Fig. 7 *F* and *G*). Taken together, Man1b1 O-glycosylation observed under our experimental conditions is likely a byproduct of the cytoplasmic tail truncation rather than a responsible factor that impairs misfolded ATZ and NHK degradation.

Discussion

Polypeptides in the endoplasmic reticulum (ER) that misfold following biosynthesis are distinguished from correctly folded proteins by protein quality-control machinery (1). The selective segregation of misfolded N-linked glycoproteins as clients for ERAD is accomplished by the removal of terminal mannose units on the N-linked oligosaccharides (10). Importantly, Man1b1 shares many characteristics that are common among a class of quality-control components that have been designated as ERAD enhancers (i.e., EDEM1, OS-9, and SEL1L) (44). For example, an elevated Man1b1 concentration is sufficient to accelerate the proteasomal-mediated intracellular degradation of misfolded proteins and can even target early folding intermediates of wild-type AAT and transferrin for this fate (17). Likewise, Man1b1 is subjected to lysosomal degradation under basal conditions (45) but is stabilized posttranslationally as part of the IRE1/XBP1 arm of the unfolded protein response (UPR) (46). However, in contrast to the bone fide group of ERAD enhancers, the Man1b1 mRNA transcript is not elevated as a component of the UPR (47).

As additional evidence that Man1b1 can function in a distinct manner as compared to the designated ERAD enhancers, our previous study demonstrated that neither the mannosidase activity nor the catalytic domain of human Man1b1 is essential for the degradation of the misfolded ERAD substrate NHK (27). In the present study, to understand the mechanism of how Man1b1 contributes to misfolded AAT degradation in a catalysis-independent manner, we generated a series of N-terminal truncations in the evolutionarily extended cytoplasmic tail and observed that Δ1 to 54 Man1b1 maintained catalytic activity demonstrated by its ability to accelerate the mannose trimming of N-linked glycans which is responsible for enhancing the rate of AAT electrophoretic migration in SDS/PAGE (48) (Fig. 4 *D*, *Top*). We discovered that amino acids 1 to 54 can play a dominant role to promote the proteasomal degradation of NHK via an unconventional system that is independent of Man1b1 catalytic activity. One unique perspective that emerges from our experimental observations is that the evolutionary extension of the cytoplasmic tail allows for the functional reassignment of Man1b1 in a manner that is indifferent to the presence of N-linked glycans on the ERAD client. Emergence of the additional ERAD client recruitment system could be extremely useful for cells to cope with an acute protein load that is often responsible for exerting ER stress. In support of this notion, several groups have identified stress-mediated alterations that allow traditional glycoprotein ERAD machinery to manage the recruitment of nonglycosylated ERAD clients (49, 50). However, to the best of our knowledge our findings represent an example in which the inherent catalytic activity of a traditional ERAD component is dispensable for promoting the emergence of an alternative misfolded protein degradation system. Furthermore, we were able to demonstrate that a suspected ERAD enhancer can promote the proteasomal degradation of misfolded protein clients in a manner that is agnostic to the existence of N-linked oligosaccharides (Fig. 5). Taken together, we propose a binary model through which Man1b1 can generate a previously unknown bifurcation in the ERAD client recruitment system capable of promoting the intracellular degradation of misfolded AAT via two different systems (Fig. 8).

The mechanism of how the Man1b1 cytoplasmic tail accelerates misfolded AAT degradation via the unconventional system remains unclear at this point. However, in a prior study, a functional γ-COP binding site was identified in the Man1b1 cytoplasmic tail that was required to promote ATZ degradation (51). This observation, plus the identification of Man1b1's colocalization with a Golgi marker (27, 43), and the detection of sialic acid units associated with Δ1 to 54 Man1b1 in the present study (Fig. 7), provides several lines of evidence that Man1b1 likely traffics through the Golgi complex and utilizes a

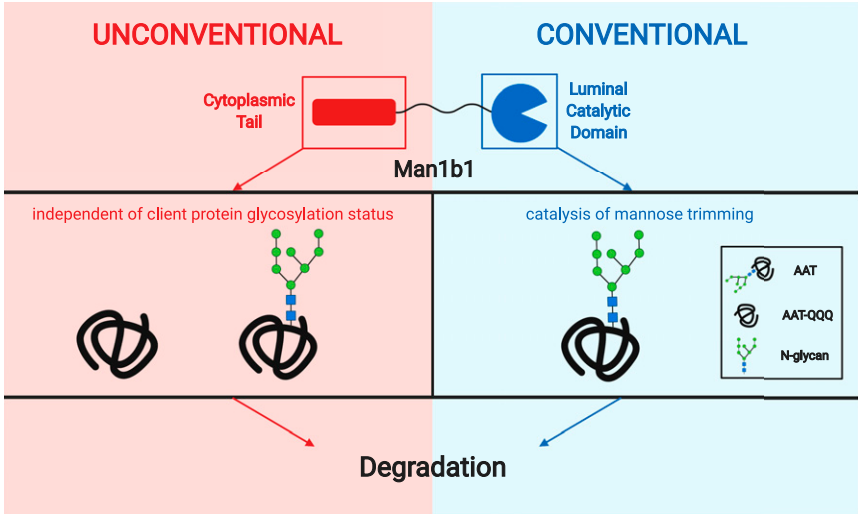

Fig. 8. Model of human Man1b1 binary functions in promoting misfolded AAT degradation. Human Man1b1 has an N-terminal cytoplasmic tail (red) and a C-terminal luminal catalytic domain (blue). Conventionally, Man1b1 is categorized as a mannosidase and carries out its function through the catalytic domain. Specifically, it catalyzes the trimming of terminal alpha-linked mannose units of N-glycans on misfolded client proteins, represented by misfolded AAT in the model. The trimming event flags AAT to be recognized by downstream pathway components leading to degradation. In our current study, we discovered the N-terminal cytoplasmic tail of Man1b1 can accelerate AAT degradation independently of its conventional catalytic function. This unconventional system occurs independently from the glycosylation status of the client proteins. Image was created with Biorender.

retrograde transport event to organize the unconventional degradation route as was previously proposed (27). We also observed a higher level of Δ1 to 54 Man1b1 protein in the lysates than WT protein under steady-state conditions (Fig. 3 *A*, *Middle*, compare lanes 2 and 3; Fig. 4 *B*, *Middle*, compare lanes 2 and 4) and performed ^{35}S metabolic pulse-chase radiolabeling to trace the fate of Man1b1 in 293T E7 cells. The analyses showed that the intracellular degradation of Δ1 to 54 Man1b1 protein was delayed compared to that of WT Man1b1 (*SI Appendix*, Fig. S5). Based on the evidence discussed above, one might speculate that Man1b1 Δ1 to 54 might lack an additional motif(s) that allow for release from the Golgi complex for proper trafficking and/or localization and therefore might enhance engagement with Golgi-situated O-glycosylation machinery (52). In order to gain a deeper level of understanding as to how the unconventional system operates, we intend to expand our studies by designing experiments that will identify potential binding partners with the cytoplasmic tail of Man1b1.

Although some might argue whether data generated from transient expression studies can faithfully identify biological mechanistic principles, our contention is that our experimental approach likely mimics the posttranslational elevation of the endogenous Man1b1 concentration as an event previously discovered to be associated with the UPR (46). In further support of our contention about the important role of Man1b1 levels, we have previously reported that the transcription up-regulation of endogenous Man1b1 levels promotes cancer cell survival in several human hepatoma cell lines (25). Whether this survival mechanism involves a switch to the unconventional ERAD client recruitment system in a manner that avoids ER stress-mediated programmed cell death will be the subject of future investigations. However, it should be noted that the tail-truncated versions of Man1b1, Δ1 to 46 and Δ1 to 54, did not elevate the levels of ER stress markers more than the expression of WT Man1b1 in 293T E7 cells (*SI Appendix*, Fig. S6), suggesting the delayed degradation rate of misfolded AAT in cells cotransfected with Δ1 to 54 Man1b1 was not due to higher ER stress levels.

In our current study, we have shown some similarity in the degradation phenotypes of the two distinct misfolded AAT variants, NHK and ATZ, in 293T E7 cells. Both variants are subjected to Man1b1 cytoplasmic tail-mediated degradation, and this unconventional degradation is independent of AAT N-glycan catalysis (Figs. 1–5). In addition, Man1b1 O-glycosylation is dispensable for both NHK and ATZ degradation mediated by Man1b1 (Fig. 7 *D*–*G*). However, considering the difference between the two variants (Fig. 1*B*), it is not surprising that differential results were also observed. First, truncation of the Man1b1 cytoplasmic tail, namely Δ1 to 54 Man1b1, was sufficient to completely ablate ATZ intracellular degradation promoted by Man1b1 (Fig. 3), but this effect was only partial on NHK (Fig. 2 *C* and *D*). Second, the N-glycan catalytic function of Man1b1 played a negligible role in ATZ degradation (Fig. 4 *D* and *E*), but was responsible for a statistically significant part of NHK degradation under steady-state conditions (Fig. 4 *B* and *C*). Although in the ^{35}S metabolic pulse-chase radiolabeling experiments the difference of NHK degradation rates between WT and D463N Man1b1 groups did not reach statistical significance, D463N Man1b1 delayed NHK degradation at all timepoints (Fig. 6*J*). The slight difference in results between the two experimental approaches could be explained by the fact that the steady-state Western blotting data represented an accumulative effect of 24-h degradation events and the radiolabeling results only reflected a 15-min-labeled population degrading over 5 h. Third, the influence of Man1b1 on ATZ degradation appeared refractory to both lactacystin and bafilomycin (*SI Appendix*, Fig. S4), but proteasomal degradation contributed to both the conventional and unconventional intracellular elimination of NHK (Fig. 6 *A*–*I*). We should note that, although ATZ polymers were reported to be degraded by lysosomes under basal conditions (53), there is the possibility that the transfected Man1b1 could degrade this population of ATZ by a recently identified bafilomycin-insensitive lysosomal pathway (54). In addition, our studies might have identified a distinct disposal system that eliminates soluble polymers or aggregates. Therefore, our observations require additional investigation as multiple intracellular ATZ populations can exist in the cell, which would complicate the interpretation of our findings. The future study might help to identify the actual toxic species responsible for the emergence of end-stage liver disease in infants which is still under intense speculation (55, 56).

Considering the redundancy of alpha-mannosidase activities capable of modifying N-glycans to promote the ERAD of misfolded glycoproteins (9, 10), it is not entirely surprising that Man1b1 might have evolved to play an additional role in higher eukaryotes independent of its mannosidase activity. This possibility is particularly evident when one considers that a single nucleotide polymorphism in the noncoding region of the human Man1b1 mRNA is able to function as a modifier that promotes severe infantile liver disease associated with alpha1-antitrypsin deficiency (AATD) (21). A central goal of future studies is to elucidate whether and how the conventional catalysis-dependent system and unconventional catalysis-independent system operate in synergy to expand a cell's ERAD capacity during the UPR to either protect, or exaggerate, the pathologies associated with numerous conformational diseases of the secretory pathway (4–7, 20, 23–25).

Materials and Methods

Details of materials regarding antibodies and other reagents such as Sialidase A, ^{35}S protein labeling mix, and inhibitors used for our study can be found in *SI Appendix*. Primers for site-directed mutagenesis PCR used in this study are listed in *SI Appendix*, Table S1. Information about expression plasmids used in all of the transient transfection experiments can also be found in *SI Appendix*. Furthermore, detailed experimental procedures for all of the techniques including cell culture, transient transfection, cell lysis, immunoblot analyses, ^{35}S metabolic pulse-chase radiolabeling, immunoprecipitation, Sialidase A treatment, multiple sequence alignment, RNA extraction, quantitative PCR technique, statistical analyses, and others can also be found in *SI Appendix*.

Data Availability. All data are included in the figures and *SI Appendix*. Raw data values obtained from all Western blots and ^{35}S metabolic pulse-chase radiolabeling experiments are available at Figshare (https://figshare.com/articles/dataset/WB_and_Pulse_Chase_Quantification_for_PNAS_Manuscript_xlsx/12869894/1) (57).

ACKNOWLEDGMENTS. We thank the Zheng laboratory (Michigan State University) for providing the 293T E7 Man1b1-knockout cell line. This work was supported by research grants from Alpha-1 Foundation, Miami, Florida (to R.N.S.).

1. D. Balchin, M. Hayer-Hartl, F. U. Hartl, In vivo aspects of protein folding and quality control. *Science* **353**, aac4354 (2016).
2. R. J. Ellis, T. J. Pinheiro, Medicine: danger–misfolding proteins. *Nature* **416**, 483–484 (2002).
3. Z. Sun, J. L. Brodsky, Protein quality control in the secretory pathway. *J. Cell Biol.* **218**, 3171–3187 (2019).
4. T. K. Chaudhuri, S. Paul, Protein-misfolding diseases and chaperone-based therapeutic approaches. *FEBS J.* **273**, 1331–1349 (2006).
5. W. E. Balch, R. I. Morimoto, A. Dillin, J. W. Kelly, Adapting proteostasis for disease intervention. *Science* **319**, 916–919 (2008).
6. D. Patel, J. H. Teckman, Alpha-1-Antitrypsin deficiency liver disease. *Clin. Liver Dis.* **22**, 643–655 (2018).
7. P. G. Needham, C. J. Guerriero, J. L. Brodsky, Chaperoning endoplasmic reticulum-associated degradation (ERAD) and protein conformational diseases. *Cold Spring Harb. Perspect. Biol.* **11**, a033928 (2019).
8. C. M. Cabral, Y. Liu, R. N. Sifers, Dissecting glycoprotein quality control in the secretory pathway. *Trends Biochem. Sci.* **26**, 619–624 (2001).
9. L. W. Ruddock, M. Molinari, N-glycan processing in ER quality control. *J. Cell Sci.* **119**, 4373–4380 (2006).

10. S. S. Vembar, J. L. Brodsky, One step at a time: Endoplasmic reticulum-associated degradation. *Nat. Rev. Mol. Cell Biol.* **9**, 944–957 (2008).
11. N. Hosokawa, Y. Kamiya, D. Kamiya, K. Kato, K. Nagata, Human OS-9, a lectin required for glycoprotein endoplasmic reticulum-associated degradation, recognizes mannose-trimmed N-glycans. *J. Biol. Chem.* **284**, 17061–17068 (2009).
12. A. Tannous, G. B. Pisoni, D. N. Hebert, M. Molinari, N-linked sugar-regulated protein folding and quality control in the ER. *Semin. Cell Dev. Biol.* **41**, 79–89 (2015).
13. C. A. Jakob, P. Burda, J. Roth, M. Aebi, Degradation of misfolded endoplasmic reticulum glycoproteins in Saccharomyces cerevisiae is determined by a specific oligosaccharide structure. *J. Cell Biol.* **142**, 1223–1233 (1998).
14. S. Jelinek-Kelly, T. Akiyama, B. Saunier, J. S. Tkacz, A. Herscovics, Characterization of a specific alpha-mannosidase involved in oligosaccharide processing in Saccharomyces cerevisiae. *J. Biol. Chem.* **260**, 2253–2257 (1985).
15. B. Henrissat, G. Davies, Structural and sequence-based classification of glycoside hydrolases. *Curr. Opin. Struct. Biol.* **7**, 637–644 (1997).
16. A. Herscovics, Structure and function of Class I alpha 1,2-mannosidases involved in glycoprotein synthesis and endoplasmic reticulum quality control. *Biochimie* **83**, 757–762 (2001).
17. Y. Wu, M. T. Swulius, K. W. Moremen, R. N. Sifers, Elucidation of the molecular logic by which misfolded alpha 1-antitrypsin is preferentially selected for degradation. *Proc. Natl. Acad. Sci. U.S.A.* **100**, 8229–8234 (2003).
18. D. S. Gonzalez, K. Karaveg, A. S. Vandersall-Nairn, A. Lal, K. W. Moremen, Identification, expression, and characterization of a cDNA encoding human endoplasmic reticulum mannosidase I, the enzyme that catalyzes the first mannose trimming step in mammalian Asn-linked oligosaccharide biosynthesis. *J. Biol. Chem.* **274**, 21375–21386 (1999).
19. L. O. Tremblay, A. Herscovics, Cloning and expression of a specific human alpha 1,2-mannosidase that trims Man9GlcNAc2 to Man8GlcNAc2 isomer B during N-glycan biosynthesis. *Glycobiology* **9**, 1073–1078 (1999).
20. G. George *et al*., EDEM2 stably disulfide-bonded to TXNDC11 catalyzes the first mannose trimming step in mammalian glycoprotein ERAD. *eLife* **9**, e53455 (2020).
21. S. Pan *et al*., Single nucleotide polymorphism-mediated translational suppression of endoplasmic reticulum mannosidase I modifies the onset of end-stage liver disease in alpha1-antitrypsin deficiency. *Hepatology* **50**, 275–281 (2009).
22. D. Rymen *et al*., MAN1B1 deficiency: An unexpected CDG-II. *PLoS Genet.* **9**, e1003989 (2013).
23. M. A. Rafiq *et al*., Mutations in the alpha 1,2-mannosidase gene, MAN1B1, cause autosomal-recessive intellectual disability. *Am. J. Hum. Genet.* **89**, 176–182 (2011).
24. T. Zhou, D. A. Frabutt, K. W. Moremen, Y. H. Zheng, ERManI (endoplasmic reticulum class I α-Mannosidase) is required for HIV-1 envelope glycoprotein degradation via endoplasmic reticulum-associated protein degradation pathway. *J. Biol. Chem.* **290**, 22184–22192 (2015).
25. S. Pan *et al*., ERManI is a target of miR-125b and promotes transformation phenotypes in hepatocellular carcinoma (HCC). *PLoS One* **8**, e72829 (2013).
26. H. F. Wang *et al*., MAN1B1 is associated with poor prognosis and modulates proliferation and apoptosis in bladder cancer. *Gene* **679**, 314–319 (2018).
27. M. J. Iannotti, L. Figard, A. M. Sokac, R. N. Sifers, A Golgi-localized mannosidase (MAN1B1) plays a non-enzymatic gatekeeper role in protein biosynthetic quality control. *J. Biol. Chem.* **289**, 11844–11858 (2014).
28. R. N. Sifers, S. Brashears-Macatee, V. J. Kidd, H. Muensch, S. L. Woo, A frameshift mutation results in a truncated alpha 1-antitrypsin that is retained within the rough endoplasmic reticulum. *J. Biol. Chem.* **263**, 7330–7335 (1988).
29. Y. Iida *et al*., SEL1L protein critically determines the stability of the HRD1-SEL1L endoplasmic reticulum-associated degradation (ERAD) complex to optimize the degradation kinetics of ERAD substrates. *J. Biol. Chem.* **286**, 16929–16939 (2011).
30. R. Huber, R. W. Carrell, Implications of the three-dimensional structure of alpha 1-antitrypsin for structure and function of serpins. *Biochemistry* **28**, 8951–8966 (1989).
31. D. A. Lomas, D. L. Evans, J. T. Finch, R. W. Carrell, The mechanism of Z alpha 1-antitrypsin accumulation in the liver. *Nature* **357**, 605–607 (1992).
32. R. N. Sifers *et al*., Tissue specific expression of the human alpha-1-antitrypsin gene in transgenic mice. *Nucleic Acids Res.* **15**, 1459–1475 (1987).
33. P. E. Stein, R. W. Carrell, What do dysfunctional serpins tell us about molecular mobility and disease? *Nat. Struct. Biol.* **2**, 96–113 (1995).
34. R. N. Sifers, M. J. Finegold, S. L. Woo, Molecular biology and genetics of alpha 1-antitrypsin deficiency. *Semin. Liver Dis.* **12**, 301–310 (1992).
35. R. N. Sifers, M. J. Finegold, S. L. Woo, Alpha-1-antitrypsin deficiency: Accumulation or degradation of mutant variants within the hepatic endoplasmic reticulum. *Am. J. Respir. Cell Mol. Biol.* **1**, 341–345 (1989).
36. J. C. Christianson, T. A. Shaler, R. E. Tyler, R. R. Kopito, OS-9 and GRP94 deliver mutant alpha1-antitrypsin to the Hrd1-SEL1L ubiquitin ligase complex for ERAD. *Nat. Cell Biol.* **10**, 272–282 (2008).
37. N. Hosokawa *et al*., Enhancement of endoplasmic reticulum (ER) degradation of misfolded Null Hong Kong alpha1-antitrypsin by human ER mannosidase I. *J. Biol. Chem.* **278**, 26287–26294 (2003).
38. J. H. Teckman, N. Mangalat, Alpha-1 antitrypsin and liver disease: Mechanisms of injury and novel interventions. *Expert Rev. Gastroenterol. Hepatol.* **9**, 261–268 (2015).
39. K. Karaveg *et al*., Mechanism of class 1 (glycosylhydrolase family 47) alpha-mannosidases involved in N-glycan processing and endoplasmic reticulum quality control. *J. Biol. Chem.* **280**, 16197–16207 (2005).
40. S. W. Mast, K. W. Moremen, Family 47 α-mannosidases in N-Glycan processing. *Methods Enzymol* **415**, 31–46 (2006).
41. K. Karaveg, K. W. Moremen, Energetics of substrate binding and catalysis by class 1 (glycosylhydrolase family 47) alpha-mannosidases involved in N-glycan processing and endoplasmic reticulum quality control. *J. Biol. Chem.* **280**, 29837–29848 (2005).
42. J. H. Cormier, T. Tamura, J. C. Sunryd, D. N. Hebert, EDEM1 recognition and delivery of misfolded proteins to the SEL1L-containing ERAD complex. *Mol. Cell* **34**, 627–633 (2009).
43. S. Pan *et al*., Golgi localization of ERManI defines spatial separation of the mammalian glycoprotein quality control system. *Mol. Biol. Cell* **22**, 2810–2822 (2011).
44. M. Hagiwara, J. Ling, P. A. Koenig, H. L. Ploegh, Posttranscriptional Regulation of Glycoprotein Quality Control in the Endoplasmic Reticulum Is Controlled by the E2 Ub-Conjugating Enzyme UBC6e. *Mol. Cell* **63**, 753–767 (2016).
45. Y. Wu, D. J. Termine, M. T. Swulius, K. W. Moremen, R. N. Sifers, Human endoplasmic reticulum mannosidase I is subject to regulated proteolysis. *J. Biol. Chem.* **282**, 4841–4849 (2007).
46. D. J. Termine, K. W. Moremen, R. N. Sifers, The mammalian UPR boosts glycoprotein ERAD by suppressing the proteolytic downregulation of ER mannosidase I. *J. Cell Sci.* **122**, 976–984 (2009).
47. H. Yoshida *et al*., A time-dependent phase shift in the mammalian unfolded protein response. *Dev. Cell* **4**, 265–271 (2003).
48. Y. Liu, P. Choudhury, C. M. Cabral, R. N. Sifers, Oligosaccharide modification in the early secretory pathway directs the selection of a misfolded glycoprotein for degradation by the proteasome. *J. Biol. Chem.* **274**, 5861–5867 (1999).
49. R. Ushioda, J. Hoseki, K. Nagata, Glycosylation-independent ERAD pathway serves as a backup system under ER stress. *Mol. Biol. Cell* **24**, 3155–3163 (2013).
50. E. Ron *et al*., Bypass of glycan-dependent glycoprotein delivery to ERAD by up-regulated EDEM1. *Mol. Biol. Cell* **22**, 3945–3954 (2011).
51. S. Pan, X. Cheng, R. N. Sifers, Golgi-situated endoplasmic reticulum α-1, 2-mannosidase contributes to the retrieval of ERAD substrates through a direct interaction with γ-COP. *Mol. Biol. Cell* **24**, 1111–1121 (2013).
52. P. Van den Steen, P. M. Rudd, R. A. Dwek, G. Opdenakker, Concepts and principles of O-linked glycosylation. *Crit. Rev. Biochem. Mol. Biol.* **33**, 151–208 (1998).
53. I. Fregno *et al*., ER-to-lysosome-associated degradation of proteasome-resistant ATZ polymers occurs via receptor-mediated vesicular transport. *EMBO J.* **37**, e99259 (2018).
54. S. Omari *et al*., Noncanonical autophagy at ER exit sites regulates procollagen turnover. *Proc. Natl. Acad. Sci. U.S.A.* **115**, E10099–E10108 (2018).
55. T. Hidvegi *et al*., An autophagy-enhancing drug promotes degradation of mutant alpha1-antitrypsin Z and reduces hepatic fibrosis. *Science* **329**, 229–232 (2010).
56. R. N. Sifers, Medicine. Clearing conformational disease. *Science* **329**, 154–155 (2010).
57. A. H. Sun *et al*, WB and pulse chase quantification for PNAS manuscript. *Figshare*. https://figshare.com/articles/dataset/WB_and_Pulse_Chase_Quantification_for_PNAS_Manuscript_xlsx/12869894/1. Deposited 26 August 2020.